Investigation into macroscopic and microscopic behaviors of wet granular soils using discrete element method and X-ray computed tomography

Vinh-Du Than[1,2,*], *Anh-Minh* Tang[1], *Jean-Noël* Roux[1], *Jean-Michel* Pereira[1], *Patrick* Aimedieu[1], and *Michel* Bornert[1]

[1] Laboratoire Navier, UMR 8205, École des Ponts ParisTech, IFSTTAR, CNRS, Université Paris-Est, France
[2] University of Danang, College of Technology, Department of Civil Engineering, Danang, Vietnam

Abstract. We present an investigation into macroscopic and microscopic behaviors of wet granular soils using the discrete element method (DEM) and the X-ray Computed Tomography (XRCT) observations. The specimens are first prepared in very loose states, with frictional spherical grains in the presence of a small amount of an interstitial liquid. Experimental oedometric tests are carried out with small glass beads, while DEM simulations implement a model of spherical grains joined by menisci. Both in experiments and in simulations, loose configurations with solid fraction as low as 0.30 are prepared under low stress, and undergo a gradual collapse in compression, until the solid fraction of cohesionless bead packs (0.58 to 0.6) is obtained. In the XRCT tests, four 3D tomography images corresponding to different typical stages of the compression curve are used to characterize the microstructure.

1 Introduction

Wet granular materials are present in Nature (e.g., partially saturated soils) and industrial processes (such as granulation). For low saturations, the appearance of water menisci creates adhesive forces which strongly affect the macroscopic material behavior. Such cohesive materials, as opposed to cohesionless ones, may form stable structures at very low density; they are sensitive to stress intensity, not only to stress direction. Characterizations of the mechanical behavior of wet granular materials or unsaturated soils are most often carried out at the macroscopic scale [1], at which the irreversible compression and decompression curves, for a material subject to varying external load intensity, play a central role. To investigate contact networks and interstitial liquid morphology, several investigation techniques suitable to unsaturated granular assemblies have been recently used: fluorescence microscopy (FM) [2] and X-ray computed tomography (XRCT) [3]. As opposed to FM techniques, which require delicate choices of both granular materials and suitable (index-matched) liquids, XRCT, a high-resolution non-destructive observation technique, does not need any sample pre-treatment.

The present work reports on results of experiments on glass beads with capillary bonds in the pendular state, subjected to oedometric compression tests and observed at small scale by XRCT. Parallel to these experiments, as the material lends itself to numerical modeling [4], DEM simulations are carried out for the same test, providing access to detailed microstructural a micromechanical information. Numerical and experimental results are presented and compared in oedometric compression cycles, both for the plastic compression curve and the evolution of coordination numbers, as well as basic geometric features.

2 Experiments

The experimental procedure consists in an oedometric compression, supplemented with the acquisition of a XRCT scan of the central part of the sample at different steps.

2.1 Material and methods

2.1.1 Material and specimen preparation

The studied material is an assembly of spherical glass beads (density 2,460 kg.m$^{-3)}$ with an average diameter of about 100 microns. To prepare the specimens the glass beads are first mixed with water. The low water content (3.5 % by mass) ensures that the material remains in at the pendular regime. The wet glass beads are then placed on a 200 μm opening sieve installed 80 mm above an oedometric cell of diameter 20 mm. This size allows passing a maximum of two grains at the same time through the grating. The sieve is vertically vibrated, so that the clusters of glass beads sequentially pass through and fall into the cell.

This procedure yields loose samples with solid fraction $\Phi_0 = 0.30$ (corresponding to void ratio $e_0 = 2.33$), with an initial height of 10 mm.

* Corresponding author: vinh-du.than@enpc.fr

2.1.2 X-ray computed tomography tests

After a first compression reduces its void ratio from the initial state (e_0 = 2.33) to the first position S1 on Fig. 3 (e_1 = 2.21), an XRCT scan is carried out to visualize only the central zone of the sample (10 mm in diameter and 8 mm in height). Fig. 1 shows an example of reconstructed 3D image obtained from such a scan (here the scan time was 240 min and the voxel size 6.5 µm).

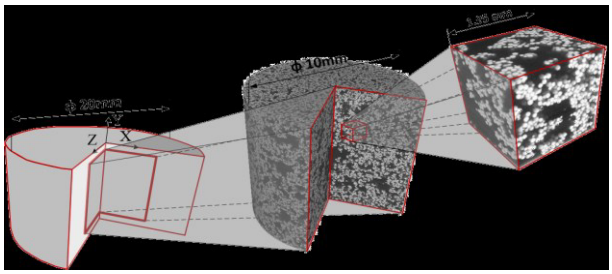

Fig. 1. Example of the position of the XRCT scan inside a sample and an example of investigated cube.

Fig. 1 clearly illustrates the ability of the XRCT technique to distinguish the grains and the pores - lighter grays characterizing larger X-ray absorption.

The same procedure is then repeated three times to obtain the XRCT images corresponding to positions marked S2 to S4 on the compression curve of Fig. 3.

2.1.3 Image processing

Image processing is carried out using software Fiji and the authors' codes, exploiting and adapting, for the detection of spherical objects, the algorithms developed by Xie *et al.* [6] (details are provided in [7].

From the 3D tomography images of the XRCT scans, cubical subregions (edge length =1.95 mm) are extracted in order to analyze the kinematics of the sample in compression. One such subdomain is shown in Fig. 1. Ten such cubes are randomly extracted at different positions within the scan, to take into account the sample microstructure heterogeneity.

Fig. 2 shows an example for one slice in a 3D detected image. The blue disks are the detected spheres, and the black points represent their centers. Incomplete white disks at the border are not used for center detection.

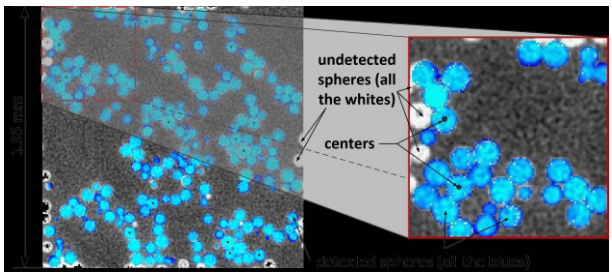

Fig. 2. A slice in a 3D detected image (not to scale).

2.2 Oedometric compression behavior

The specimen is carefully placed on the loading platform of the oedometric compression cell. The cell is then moved upward at a speed of 0.5 mm/min, towards a fixed piston where the vertical force is measured. Tests are duplicated to assess reproducibility.

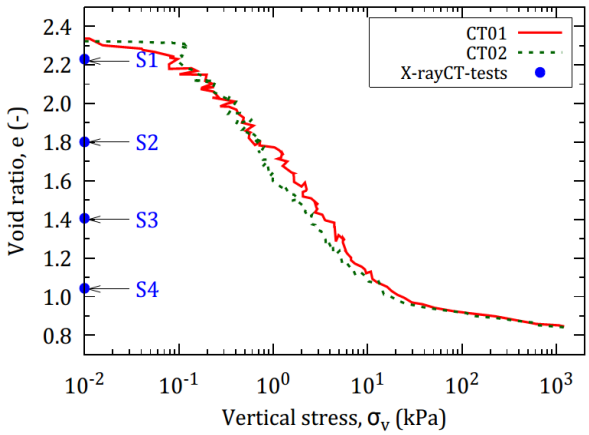

Fig. 3. Void ratio versus vertical stress during oedometric compression tests (CT01 and CT02). The circle points show the positions of XRCT scans.

Fig. 3 illustrates the compression curves for two different specimens (CT01 and CT02). Based on the shape of these curves and on the range of vertical stress, three stages, with the void ratio decreasing slowly in the first one, under low stress (< 0.1 kPa), then faster in the second one, and slowly again, in the third stage, at high stress (> 10 kPa). Blue dotes marked S1, S2, S3, and S4 show the *e* values of the XRCT scans.

2.3 Grain-scale analysis

2.3.1 Heterogeneity

The number of particles detected within the ten cubes at each of the four steps Si (i = 1 to 4) are shown in Fig. 4. These numbers increase with density, from approximately 4000 on average in the loosest state S1 (*e* = 1.04) to about 7500 in the densest one, S4 (*e* = 1.04).

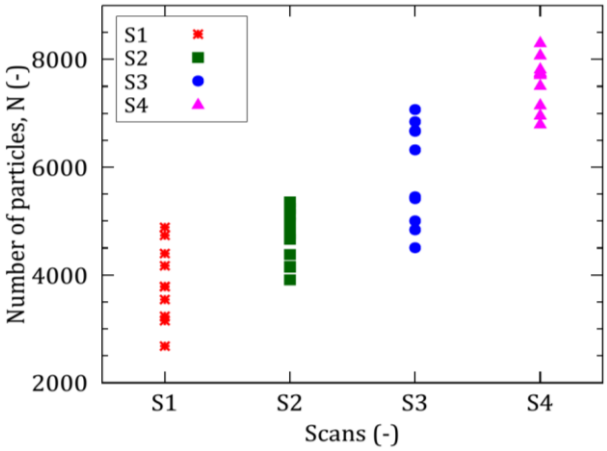

Fig. 4. Number of particles of the ten cubes for four steps after detection process.

The resulting solid fraction (averaged over all ten cubes) is compared in Fig. 5 to the macroscopic value (corresponding to the void ratio in Fig. 3). The average values are directly calculated from the tomography images, based on the IsoData method [8], applied to the segmentation process. In addition, after the detection process, the solid fraction is easily computed by dividing

the volume of all the particles by the volume of the cube. The resulting differences between different values characterizes the heterogeneity of the microstructure of the sample. The obtained solid fraction is smaller after the detection process than before, decreasing respectively by 0.05, 0.06, 0.07, and 0.1 for scans S1, S2, S3, and S4.

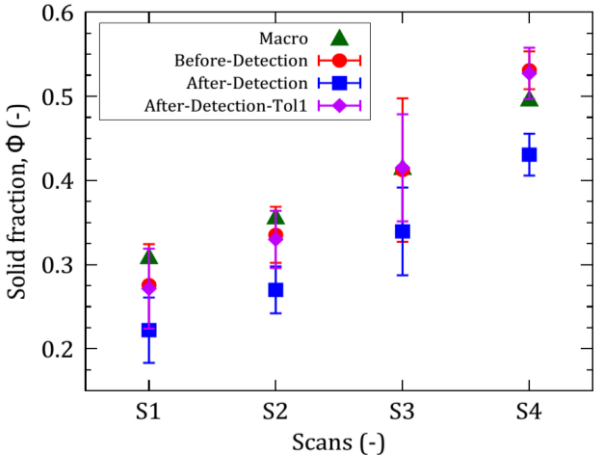

Fig. 5. Macroscopic solid fraction (triangle) and the average solid fraction of 4 steps before and after the detection process with tolerance of 0 and 1 voxel.

However, if it is recalculated with a tolerance of 1 voxel (6.5 μm) added to the diameter of the spheres the results come very close to the values obtained before detection. A tolerance of 1 voxel in all post-detection analysis thus appears quite suitable.

2.3.2 Total coordination number

We denote the coordination number by z. While it should represent the average number of contacts per grain, the finite resolution of the XRCT method, in the present case for which the particle diameter is only about 12 to 14 times as large as the voxel size, forbids a clear distinction between contacting and close neighbors.

Consequently, we compute z with a finite tolerance in terms of apparent interparticle distance.

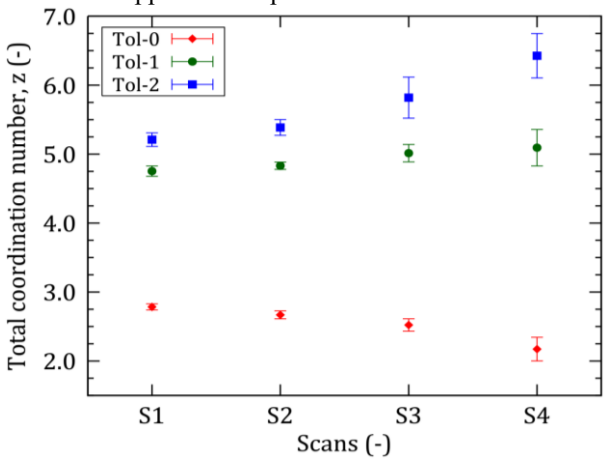

Fig. 6. Total coordination numbers of 4 steps with three values of tolerance (0, 1 and 2 voxels).

Fig. 6 shows the average coordination number at the four compression steps for three values of this tolerance (0, 1, and 2 voxels). The apparent value of z decreases under growing stress for tolerance zero, but measured z values are much larger (and realistic) as the tolerance is increased. The error bars are wider at a denser state or with a higher tolerance. The tolerance of 1 voxel is chosen for all calculations, this value is close to the one obtained in [9].

3 DEM simulations

3.1 Model material

The simulated systems are assemblies of equal-sized spherical beads of diameter a, interacting in their contacts by Hertz-Mindlin elastic-frictional forces, with the elastic properties of glass and friction coefficient 0.3.

As in Refs. [5,10], liquid menisci, with a fixed volume V_m, are assumed to form in contacting grains, with a rupture distance $V_m^{1/3}$ frictional. The capillary force is computed using the Maugis approximation [5,10]. Most calculations are carried out with the dimensionless meniscus volume $V_m/(a^3) = 10^{-3}$ [5].

3.2 Specimen preparation and compression process

A hard sphere event-driven method is first used to prepare disordered, low density configurations of 4000 grains. All particles are then launched with Gaussian-distributed random velocities with quadratic mean V_0. They collide and stick to one another within a cell of constant size, forming larger and larger aggregates. Finally, all grains are connected to one another by cohesive contacts and reach an equilibrium position.

The final packing structures are oedometrically compressed within periodic cells under growing axial stress. A stepwise pressure loading path is applied. In each compression step, vertical pressure σ_v is multiplied by a constant factor $10^{1/4}$, and one waits until the new equilibrium configuration is reached. The compression program is pursued until σ^{max}_v (maximum value $2x10^3$ kPa), well beyond complete plastic collapse is obtained. Upon decompression (not shown here), the system approximately keeps the highest density achieved under growing stress [4,5].

3.3 Compression curve and coordination number

The result of numerical oedometric compression is shown in Fig. 7, for an initial solid fraction Φ_0=0.30, as the conventional soil mechanics plot of e versus $\log(\sigma_v)$.

Three regimes can be identified in the compression curve, depending on the range of vertical stress σ_v [5]. Under low vertical stress σ_v, the initial structure can sustain the increasing stress without rearrangement and void ratio e remains nearly constant. The second regime starts as the void ratio starts to sharply decreases, due to the gradual collapse of the initial structure. Finally, void ratio e, in a third regime, approaches a minimum value e_{min}, which characteristics a structure stable without capillary cohesion. As in other models of cohesive

granular systems [4], the collapse is controlled by the ratio of the applied stress to the characteristic stress built with the tensile strength of menisci and the particle diameter [5].

The coordination number z, is the sum of the contact coordination number z_c and the coordination number of distant interactions, through menisci joining non-contacting grains, z_d.

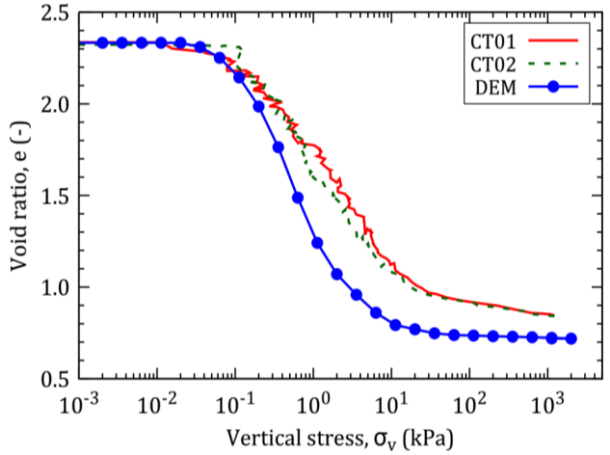

Fig. 7. Void ratio as a function of vertical stress σ_v. The circle-blue curve denotes the DEM's result. The continuous and dashed lines (CT01, 02) denote the results of oedometric tests.

Fig. 8 plots z, z_c, z_d versus vertical stress σ_v in the compression cycle and the total coordination number z in XRCT tests versus positions of scans. These positions are directly interpolated from the compaction curve of the DEM in Fig. 3. Initially, one has $z_d = 0$, because the gentle aggregation process, in that case, does not allow contact opening. z_c and z_d remain unchanged in the first regime. Both coordination numbers start to increase as the structure collapses and reorganizes in the second regime. They exhibit little change in the third regime, showing that the increase of the number of contacts is mainly due to the closing of narrow gaps between pairs of grains joined by a meniscus, as the structure is further compressed - a moderate effect.

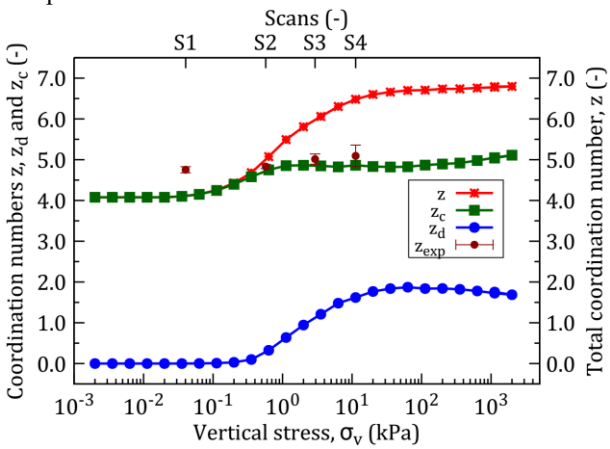

Fig. 8. Coordination number z, z_c and z_d versus vertical stress and the total coordination number z versus positions of scans.

A comparison with the total coordination number z measured in the experiment is also shown in Fig. 8, for the values of stress corresponding the scan positions. In general, the order of magnitude and the general trend of z_{exp} are well captured. We obtained a fairly good agreement of z_{exp} for the number of contacts z_c.

4 Conclusions

These results show that very loose, yet stable, states of wet granular assemblies can be prepared and subjected to mechanical tests, using very small water content. Oedometric tests reveal very similar behaviors in DEM simulations and in experiments. The same three stages of compression curve of cohesive soils are observed. Encouraging similarities are also observed in coordination number values as obtained through XRCT investigations of the microstructure and in DEM simulations. Microtomographic measurements enable assessments of sample homogeneity.

Acknowledgments

The first author is supported by the Scholarship of Ministry of Education and Training – Vietnam (the Project No 911) to do this work.

References

[1] D. M. Wood, *Soil Behaviour and Critical State Soil Mechanics* (Cambridge University Press, 1990).
[2] T. G. Mason, A. J. Levine, D. Ertaş, and T. C. Halsey, Phys. Rev. E **60**, R5044 (1999).
[3] J.-F. Bruchon, J.-M. Pereira, M. Vandamme, N. Lenoir, P. Delage, and M. Bornert, Granul. Matter **15**, 783 (2013).
[4] F. Gilabert, J.-N. Roux, and A. Castellanos, Phys. Rev. E **78**, 031305 (2008).
[5] V.-D. Than, S. Khamseh, A.-M. Tang, J.-M. Pereira, F. Chevoir, and J.-N. Roux, J. Eng. Mech. C4016001 (2016).
[6] L. Xie, R. E. Cianciolo, B. Hulette, H. W. Lee, Y. Qi, G. Cofer, and G. A. Johnson, Toxicol. Pathol. **40**, 764 (2012).
[7] V.-D. Than, P. Aimedieu, M. Bornert, J.-M. Pereira, J.-N. Roux, and A.-M. Tang, Eur. Phys. J. E (to be published).
[8] T. W. Ridler and S. Calvard, IEEE Trans. Syst. Man Cybern. **8**, 630 (1978).
[9] T. Aste, M. Saadatfar, and T. J. Senden, J. Stat. Mech. Theory Exp. **2006**, P07010 (2006).
[10] S. Khamseh, J.-N. Roux, and F. Chevoir, Phys. Rev. E **92**, 22201 (2015).